International Journal of Biological Macromolecules 233 (2023) 123545

Contents lists available at ScienceDirect

International Journal of Biological Macromolecules

journal homepage: www.elsevier.com/locate/ijbiomac

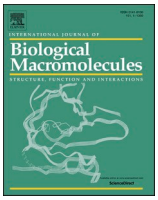

Engineering a DNA polymerase from *Pyrobaculum calidifontis* for improved activity, processivity and extension rate

Shazeel Ahmad [a,1], Syed Farhat Ali [b,1], Saima Iftikhar [a], Naeem Rashid [a,*]

[a] School of Biological Sciences, University of the Punjab, Quaid-e-Azam Campus, Lahore 54590, Pakistan
[b] KAM-School of Life Sciences, Forman Christian College (A Chartered University), Ferozepur Road, Lahore 54600, Pakistan

ARTICLE INFO

Keywords:
Pyrobaculum calidifontis
Family-B DNA polymerase
Processivity
Fidelity
Extension rate
3′-5′ exonuclease activity

ABSTRACT

Positively charged amino acids in the DNA polymerase domain are important for interaction with DNA. Two potential residues in the palm domain of *Pca*-Pol, a DNA polymerase from *Pyrobaculum calidifontis*, were identified and mutated to arginine in order to improve the properties of this enzyme. The mutant proteins were heterologously produced in *Escherichia coli*. Biochemical characterization revealed that there was no significant difference in pH, metal ion, buffer preferences, 3′ − 5′ exonuclease activity and error rate of the wild-type and the mutant enzymes. However, the specific activity, processivity and extension rate of the mutant enzymes increased significantly. Specific activity of one of the mutants (G522R-E555R) was nearly 9-fold higher than that of the wild-type enzyme. These properties make G522R-E555R mutant enzyme a potential candidate for commercial applications.

1. Introduction

DNA polymerase carries out template-guided synthesis of DNA. The enzyme functions in the presence of divalent cations (typically Mg^{+2}). Positively charged amino acids of the enzyme are important for DNA binding [1]. DNA polymerases are used for a variety of applications including routine PCR, error-prone PCR, isothermal amplification, site-directed mutagenesis and DNA sequencing [2,3]. Both engineered and natural DNA polymerases are also used in synthetic biology as they can accept modified DNA substrates and can be used for propagation of an artificial genetic system [4,5]. Moreover, DNA polymerases are also important targets for treatment and prevention of diseases like cancer [1].

Based on the primary structure, DNA polymerases are classified into seven families namely A, B, C, D, X, Y and RT [6]. Family B DNA polymerases are found in all domains of life [7]. Many family B DNA polymerases have been reported from archaea [8,9]. Most of these belong to the phylum Euryarchaeota including *Thermococcus gammatolerans* [10], *Thermococcus gorganarius* [11], *Thermococcus kodakarensis (Tko)* [12], *Thermococcus eurythermalis* [13] and *Pyrococcus furiosus (Pfu)* [14]. However, relatively less have been characterized from Crenarchaeota - *Pyrobaculum calidifontis* [15,16] and *Sulfolobus solfataricus* [17] – to name a few.

The DNA polymerases from *T. kodakarensis* and *P. furiosus* have suitable properties for PCR application and are commercially available as well [18]. The DNA polymerase from *T. kodakarensis* displays better processivity, extension rate and fidelity. The presence of multiple positively charged residues at the forked point is considered a key factor for its remarkable properties [19]. Also, when the polymerase domain of the low processivity *P. furiosus* DNA polymerase was replaced by the highly processive *T. kodakarensis* counterpart, it increased the processivity of the resulting chimeric enzyme [20]. Thus signifying better performance of *T. kodakarensis* DNA polymerase.

The family B DNA polymerase from the hyperthermophilic archaeon *P. calidifontis* (*Pca*-Pol) has been cloned and characterized [16,21], and its crystal structure has been determined [15]. *Pca*-Pol can be used to amplify DNA by PCR (16). However, this enzyme exhibits lower processivity. In order to improve the characteristics of this enzyme, its structure was compared with those of highly efficient DNA polymerases being used in PCR. Two amino acid residues (Gly 522 and Glu 555) in *Pca*-Pol were identified by this analysis which corresponded to positively charged amino acids in the pocket of palm domain involved in DNA binding and metal ion interaction in *Tko* DNA polymerase. So, these amino acids were mutated to arginine and corresponding single

* Corresponding author.
E-mail address: naeem.ff.sbs@pu.edu.pk (N. Rashid).
[1] Shazeel Ahmad and Syed Farhat Ali contributed equally and, in their opinion, should be considered joint first author.

https://doi.org/10.1016/j.ijbiomac.2023.123545
Received 12 October 2022; Received in revised form 20 January 2023; Accepted 31 January 2023
Available online 3 February 2023

and double mutant variants were produced. Here we report the consequent improvements in the properties of these mutants including enzyme activity, processivity and extension rate which resulted in better PCR performance.

2. Materials and methods

2.1. In-silico mutagenesis and analysis of mutants

The structure of *Pca*-Pol (PDB ID 5MDN) was used for *in-silico* analysis of mutants [15]. *In-silico* mutagenesis was done by Modeller 10.2 using "mutate_model.py" script [22]. The wild-type and mutant models were analyzed for salt bridges and hydrogen bonds by using ESBRI [23] and VADAR [24], respectively. In order to generate a model of the *Pca*-Pol and its mutants with DNA, its palm and thumb domains were individually fitted to those of *T. kodakarensis* (PDB ID 4K8Z) [12] followed by addition of DNA. The stability of the mutants was analyzed by FoldX [25].

2.2. Site-directed mutagenesis and construction of recombinant plasmids

The palm domain of *Pca*-Pol was aligned with those of other archaeal counterparts. Gly522 at forked point and Glu555 near the metal-binding aspartate of *Pca*-Pol aligned with positively charged amino acids of *T. kodakarensis* DNA polymerase and were selected to be replaced by arginine. Overlap extension PCR was performed to produce three mutants including single mutants G522R, E555R and double mutant G522R-E555R. The sequences of external and internal overlapping primers are given in Table 1. PCR amplified mutant genes were cloned in pET-21a (+) expression vector. The corresponding recombinant plasmids were named as pET-G522R, pET-E555R and pET-G522R-E555R. Sequencing of the cloned genes was done to confirm the mutants.

2.3. Gene expression and protein purification

E. coli BL21-CodonPlus(DE3)-RIL cells were transformed for expression of mutant genes. Heterologous gene expression was induced with 0.2 mM IPTG and the cultures were incubated in shaking incubator at 37 °C for ~4 h. Un-induced cells of each culture were used as a control. The resulting cultures were centrifuged and cell pellets were suspended in 25 mM Tris-Cl buffer pH 8.5. Cells were lyzed by sonication (Vibra Cell 130 VC). Soluble fractions were separated by centrifugation at 6000 ×*g* for 10 min. The recombinant proteins were partially purified by heating the soluble fractions in water bath at 80 °C for 20 min to remove heat labile *E. coli* proteins. These heated fractions were centrifuged at 12,000 ×*g* for 15 min to obtain heat-stable soluble fraction. The mutant recombinant proteins were further purified by HiTrap™ Heparin HP Column (GE Healthcare) using Äkta Purifier FPLC system (GE Healthcare). After equilibration with 25 mM Tris-Cl pH 8.5 (containing 1 mM EDTA, 2 % glycerol and 1 % β-mercaptoethanol), the heat-stable fractions were loaded onto the column, washed and eluted with a linear gradient of elution buffer (0 to 1 M NaCl in equilibration buffer). The fractions containing the recombinant protein were pooled and dialyzed against dialysis buffer (10 mM Tris-Cl pH 8.5, 25 % glycerol, 0.1 % Tween 20 and 0.2 mg/mL BSA). Protein concentration was determined by Bradford method [26].

2.4. Optimization of PCR

Buffer concentration, pH and $MgCl_2$ concentration were optimized during PCR. The PCR reaction mixture, in 25 μL, contained 100 μM each dNTP, various concentrations of $MgCl_2$, 0.2 μg template DNA, 50 pmol of each forward and reverse primers, Tris-Cl buffer (of various concentrations and pH) and the purified recombinant enzyme (0.1–2.0 μg). For pH optimization, PCR was performed at various pH of Tris-Cl buffer (7.0, 7.5, 8.0, 8.5, and 9.0) keeping the buffer concentration constant at 30 mM. For optimization of buffer concentration, PCR was performed at various concentrations of Tris-Cl buffer (10, 20, 40, 60 and 80 mM) of pH 8.0. For optimizing $MgCl_2$ concentration, PCR was performed by using 0, 1, 2, 4, 6, 8 and 10 mM of $MgCl_2$ in 30 mM Tris-Cl buffer pH 8.0. To determine the extension rate, the extension step in PCR was performed in optimized conditions for various time intervals (12–40 s) to amplify a 0.8 kb product. PCR temperature profile was: initial denaturation at 95 °C for 3 min followed by 25 cycles of denaturation at 95 °C for 30 s, primer annealing at 55 °C for 30 s and extension at 72 °C for 45 s per kb [16].

2.5. DNA polymerase activity assay

DNA polymerase activity was assayed as described previously [16]. Briefly, the reaction mixture (30 μL) consisted of 200 μM each dNTP, 2 mM $MgCl_2$, 1–8 μg activated calf thymus DNA as template (Sigma Aldrich), 4 % glycerol, 0.4 % Tween20, 2 μg/mL BSA, 20–80 mM Tris-Cl (pH 8.0) and 0.5 μCi [methyl ^{3}H]-TTP. The reaction mixture was pre-incubated at 75 °C for 3 min and then 0.1–2 μg of recombinant enzyme was added to start the reaction. Aliquots, 5 μL, were withdrawn after regular intervals (2, 4, 6 and 8 min), added to DE-81 filter discs and dried. The discs were washed thrice with 0.5 M sodium phosphate buffer (pH 7.0) followed by washing with 70 % ethanol. The discs were dried and added to vials containing 3 mL of scintillation fluid. Incorporation of radioactivity was measured as counts/min (cpm) by using Raytest Malisa scintillation counter (Berlin, Germany). One unit of DNA polymerase activity was defined as the amount of the enzyme required to incorporate 10 nmol [^{3}H]TTP into a polynucleotide fraction (adsorbed on DE-81 filter disc) at 75 °C in 30 min. The specific activity was calculated by using the following formula.

$$Specific\ activity = \frac{nmol}{78\ \mu Ci} \times \frac{Stock\ \mu Ci}{Stock\ cpm} \times \frac{Sample\ cpm}{Enzyme\ amount} \times \frac{dNTPs\ conc}{3H\text{–}dTTP\ \text{conc}}$$

2.6. Processivity assay

Processivity measurement was done by using FAM-labeled primer. The reaction mixture (20 μL) consisted of 125 μM of each dNTP, 2 mM $MgCl_2$, 100 nM template (M13mp18 ssDNA), 1 mM 5′-FAM labeled primer (5′-GCATCGGAACGAGGGTAGCAACGG), 4 % glycerol, 0.4 % Tween 20, 2 μg BSA and 20–80 mM Tris-Cl (pH 8.0). The reaction mixture was incubated in water bath at 90 °C for 3 min and then allowed to cool slowly to 55 °C for primer annealing. The recombinant enzyme 0.1–2.0 μg was added to the reaction mixture for polymerization and mixture was incubated at 72 °C for 10 s. The reaction was stopped by

Table 1
Sequence of primers used for mutagenesis by overlap extension PCR.

Enzyme	Substitution	Primer	Sequence (5′-3′)
G522R	Gly to Arg	G522R-F	TTAGGCTGGGTTCGTGCGCGGTGGTACAAG
		G522R-R	TACCACCGCGCACGAACCCAGCCTAAGTAG
E555R	Glu to Arg	E555R-F	AGGCTTGGCATCCGTGTGATATACGGCGACACGG
		E555R-R	GCCGTATATCACACGGATGCCAAGCCTCTTCGC
Wild-type	–	External-F	CATATGAGGTTTTGGCCTCTAGACGCCACGTACTCTG
		External-R	GCAGAAACTAGCCTAGGAAGTCCAAGAGTG

adding 100 μM EDTA. Fragment analysis was performed to analyze the processivity of each mutant using ABI 3500 Genetic Analyzer (Applied Biosystems). The peaks of electropherogram traces of each enzyme (wild type and mutants) were plotted on a log scale [27].

2.7. 3′-5′ Exonuclease activity assay

Assay for 3′-5′ exonuclease activity of the wild-type and mutant enzymes was done as described earlier [16]. Firstly, 3′ labeled DNA substrate was prepared. *Hin*dIII digested λ phage DNA was filled in by *exo*-deficient Klenow fragment in a reaction mixture containing 100 μM each of dATP, dGTP, dCTP and 1 μCi [methyl-^{3}H]-TTP. After radio-labeling, purification of the substrate DNA was done by sephadex G 25 spin column (GE healthcare). The assay mixture for 3′ → 5′ exonuclease activity, in 50 μL, contained 4 mM $MgCl_2$, 1 % glycerol, 0.4 % Tween20, 8 μg BSA, 20–80 mM Tris-Cl (pH 8.0) and labeled substrate DNA. The reaction mixture was pre-incubated at 75 °C for 5 min before the addition of 1 μg of each recombinant enzyme. Aliquots were removed from the reaction mixture after various time intervals and added to DE-81 filter paper discs. The discs were washed as described in the DNA polymerase assay and remaining radioactivity on the discs was measured to determine the exonuclease activity.

2.8. Fidelity assay

The fidelity of wild-type and mutant enzymes was determined by using a modification of method reported [28,29]. Briefly, pUC19 plasmid was amplified by PCR using the forward (5′-GCTACAGAGTTCTTGAAGTGGTGGCCTAAC-3′) and the reverse (5′-ACCGCCTACATACCTCGCTCTGCTAATCCT-3′) primers. The reaction mixture (50 μL) consisted of 2 mM $MgCl_2$, 20–80 mM Tris-Cl buffer, 0.5 mM dNTPs, 5 μg BSA, 0.4 % Tween 20, 1 % glycerol, 250 ng template DNA (pUC19), 100 pmol each primer and 1 μg of the recombinant DNA polymerase. PCR temperature profile was: initial denaturation at 95 °C for 3 min, followed by 30 cycles of denaturation at 95 °C for 30 s, primer annealing at 55 °C for 30 s and extension at 72 °C for 2 min. The amplified plasmid was analyzed by agarose gel electrophoresis, treated with *Dpn*I and purified. *E. coli* DH5α competent cells were transformed with purified amplified plasmid and blue-white screening was performed on LB agar plates containing IPTG and X-gal. The error rate (ER) of the wild-type and mutant enzymes was calculated by using the following formula:

$$Error\ rate = \frac{mf}{bp \times d}$$

Where mf is the mutation frequency which is the ratio of white mutant colonies to the total colonies; bp is the number of amplified base pairs of *LacZα* part of pUC19 plasmid (321 bp) and d is the template doubling 2^d (d = Amount of PCR product/amount of starting target).

2.9. Densitometry of amplified product and statistical analysis

After agarose gel electrophoresis, gel images were captured by using Chemi Doc™ XRS+ System (Bio-Rad) and analyzed with Image Lab™ Software (Bio-Rad) for quatification. All experiments were done in triplicates. One way analysis of variance (ANOVA) was done using Microsoft Excel. A p value less than 0.05 was considered statistically significant.

3. Results

3.1. In-silico analysis of mutants

Positively charged amino acids in the palm domain of DNA polymerases are important for DNA polymerase activity and processivity [19]. Multiple sequence alignment was generated among selected crenarchaeal and euryarchaeal family B DNA polymerases (Fig. 1A). This alignment revealed that Gly522 and Glu555 of *Pca*-Pol aligned with positively charged amino acids of *T. kodakarensis*. Hence, Gly522 and Glu555 in the palm domain of *Pca*-Pol were mutated to arginine residues both as single and double mutants. Fig. 1B shows these selected wild-type residues in the structure of *Pca*-Pol (PDB ID 5MDN).

After *in-silico* mutagenesis, the mutant models were analyzed. Gly522 (which corresponds to Arg501 of KOD DNA polymerase and lies at the fork point) was mutated to Arg. The side chain of Arg522 was found to be approaching DNA at the fork point. It was found that this side chain protruded nearly 3.5 Å toward DNA as compared to wild-type Gly522 (Fig. 1C). So, this can have a stabilizing effect on DNA binding and contribute to improved properties of the mutant enzyme. Glu555 corresponded to conserved positively charged amino acids of other archaeal DNA polymerases and, hence, was mutated to Arg555. When analyzed for their stability by using FoldX, these mutants were found to be stable (free energy change of −0.02 for G522R mutant and − 0.04 for E555R mutant; as compared to the wild type).

3.2. Cloning and sequencing

Based on the results of *in-silico* analysis of the selected mutants, site-directed mutagenesis of *Pca*-Pol was done. Overlap extension PCR, using mutation specific primers (Table 1), resulted in amplification of the mutant genes (Fig. S1A). These mutant genes were cloned in pET-21a (+), and named as pET-G522R, pET-E555R and pET-G522R-E555R. Digestion of the resulting recombinant plasmids with *Nde*I and *Hin*dIII liberated nearly 2.4 kb DNA fragment from the vector (corresponding to the size of *Pca-pol* gene) (Fig. S1B) indicating the cloning of the PCR amplified mutant genes. The mutations were confirmed by DNA sequencing (Fig. S2).

3.3. Production and purification of mutants

E. coli BL21-CodonPlus(DE3)-RIL cells were transformed using pET-G522R, pET-E555R and pET-G522R-E555R recombinant plasmids individually. Induction of the cells with 0.2 mM IPTG resulted in the production of nearly 89 kDa protein band, corresponding to the size of *Pca*-Pol. Analysis of the soluble and insoluble fractions, after cell lysis and centrifugation, showed that all the three recombinant mutant proteins were present in the soluble fractions. After heat-treatment of these fractions at 80 °C, all three mutant proteins remained soluble. These resulting proteins fractions were applied to HiTrap Heparin column. The mutant proteins were purified to considerable level of purity as demonstrated in Fig. 2.

3.4. Characterization of mutant enzymes

The mutant enzymes, after HiTrap Heparin column chromatography, were characterized and compared. Optimal buffer concentration and pH, $MgCl_2$ concentration, extension ability, DNA polymerase activity, 3′-5′ exonuclease activity and fidelity were determined.

3.4.1. Comparison of PCR performance of mutants

Performance of the mutants was monitored in PCR and was compared to that of the wild-type *Pca*-Pol [16]. G522R, E555R and G522R-E555R mutants did not show any difference in optimal buffer pH. All the mutants and the wild-type enzyme were optimally active at pH 8.0 (Fig. 3A). However, they displayed a slight difference in optimal buffer concentration. The single mutants, G522R and E555R, displayed a variation. They optimally amplified DNA fragments in PCR at 60–80 mM Tris-Cl (pH 8.0) in contrast to the wild-type where no amplification was achieved at this concentration. However, the buffer preference for the double mutant G522R-E555R was similar as that of the wild-type enzyme. Both of these enzymes were optimally active at 20 mM Tris-Cl pH 8.0 (Fig. 3B). When $MgCl_2$ concentration was compared, G522R

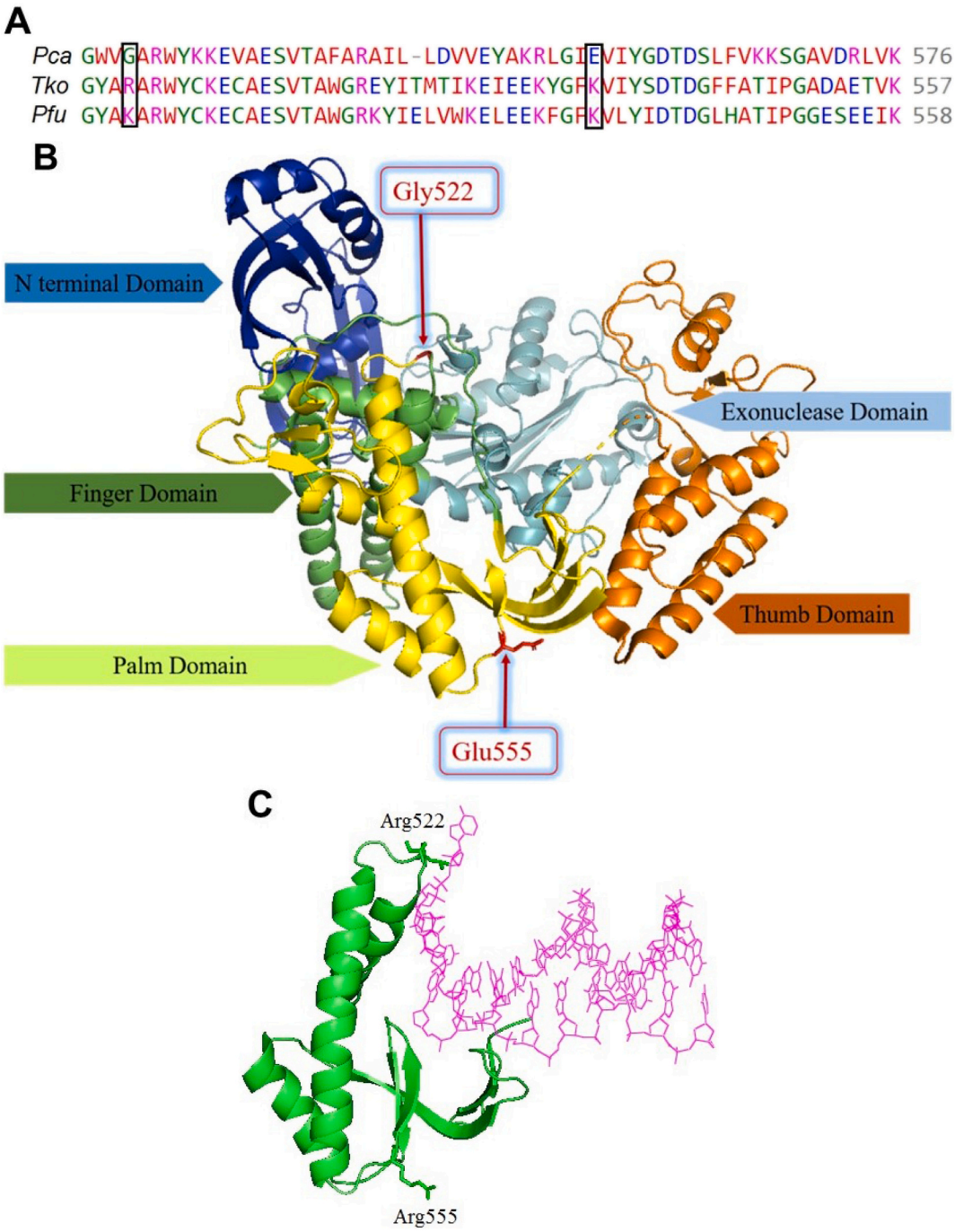

Fig. 1. A) Sequence alignment showing partial region of palm domain of *Pca*-Pol (*Pca*) PDB ID 5MDN aligned with palm domains of DNA polymerases from *T. kodakarensis* (*Tko*) PDB ID 4K8Z and *P. furiosus* (*Pfu*) PDB ID 4AIL. *Pca*Gly522 and *Pca*Glu555 aligned with positively charged residues of other DNA polymerases are outlined. B) The tertiary structure of wild-type *Pca*-Pol (PDB ID 5MDN) showing the N-terminal, exonuclease, fingers, palm and thumb domains. Gly522 and Glu555 residues selected for mutagenesis are shown. C) Selected region of palm subdomain (green) of *Pca*-Pol double mutant showing Gly522Arg and Glu555Arg (sticks) mutations with DNA (magenta).

displayed highest amplification in the presence of 4 mM $MgCl_2$, similar to the wild-type. The other two mutants, E555R and G522R-E555R, displayed highest amplification in the presence of 2 mM $MgCl_2$ (Fig. 3C).

Polymerization efficiency of the wild-type and the mutant enzymes was compared at different extension times in PCR ranging from 12 to 40 s. The wild-type enzyme requires minimum of 30 s to amplify a 0.8 kb product to a detectable level. Whereas G522R mutant required at least 18 s of extension time to amplify this fragment. Similarly, E555R mutant could amplify this product with a minimum extension time of 22 s. The double mutant, G522R-E555R, was able to amplify this DNA fragment even at an extension time of 12 s (Fig. 4, panels A, B, C and D). PCR amplification of double mutant G522R-E555R was also compared to those of *Pfu* and *Taq* DNA polymerases. It was found that G522R-E555R showed PCR amplification comparable to *Pfu* and *Taq* DNA polymerases (Fig. 4, panel E). No significant difference in amplification was observed when extension time was 1 min per kb for *Taq* and G522R-E555R DNA polymerases and 2 min per kb for *Pfu* enzyme (as recommended by the manufacturer).

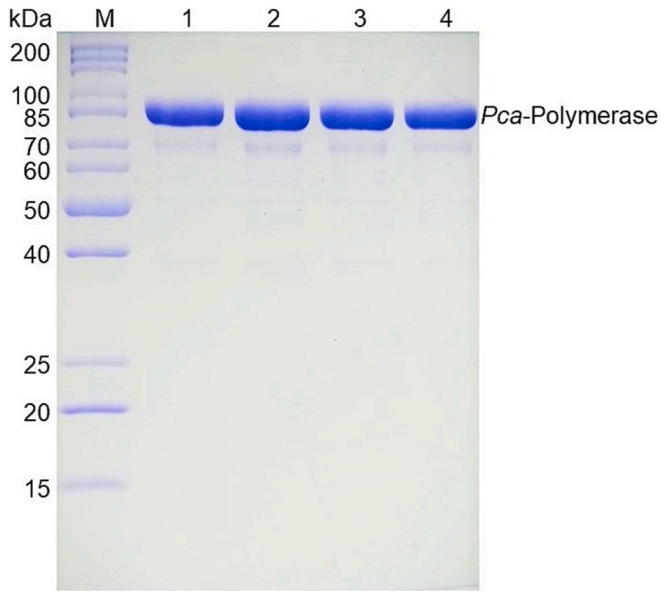

Fig. 2. Coomassie brilliant blue stained SDS-PAGE showing purified wild-type *Pca*-Pol and its mutants (~89 kDa). Lane M, protein molecular mass marker; lane 1, wild-type *Pca*-Pol; lane 2, single mutant G522R; lane 3, single mutant E555R; lane 4, double mutant G522R-E555R.

3.4.2. Comparison of DNA polymerase activity

DNA polymerase activity of wild-type *Pca*-Pol and its mutants was determined by measuring the incorporation of [methyl ^{3}H]-TTP in template DNA. The specific activity of E555R, G522R and G522R-E555R mutant enzymes was 2, 5.4 and 9.4-fold higher than that of the wild-type enzyme, respectively (Fig. 5). The specific activity of G522R-E555R was also compared with those of commercially available *Pfu* and *Taq* DNA polymerases by using the same amount of the enzymes. The determined specific activities of G522R-E555R, *Pfu* and *Taq* DNA polymerases were nearly 10,000, 8600 and 15,700 U/mg, respectively.

3.4.3. Processivity analysis

Processivity of the mutant enzymes was compared to that of the wild-type *Pca*-Pol. Processivity was determined at minimum extension time and DNA polymerase concentration to identify single hit condition. The electropherogram traces with and without various DNA polymerases are shown in Fig. 6A. Microscopic processivity (P) values were determined by analyzing the lengths (in nucleotides) and intensity of peaks of fragments extended by each enzyme. Each value of microscopic processivity was obtained by linear regression as shown in Fig. 6B and average primer extension was calculated from $1/1 - P$. The average primer extension lengths for *P. furiosus* (*Pfu*) DNA polymerase, *Pca*-Pol, E555R, G522R and G522R-E555R DNA polymerases were calculated as 6, 9, 12, 23 and 38 nucleotides, respectively (Table 2). Although both the single mutants displayed an increase in processivity as compared to the wild-type, highest increase (more than 4-fold) was observed in case of double mutant G522R-E555R. KOD DNA polymerase, however, has been reported to have a processivity of more than 300 bases [30], a value much higher than those of the double mutant G522R-E555R and *Pfu* DNA polymerase.

3.4.4. 3′-5′ exonuclease activity

DNA polymerases having 3′-5′ exonuclease activity can correct errors during DNA synthesis by removing misincorporated nucleotides. 3′-5′ exonuclease activity of wild-type *Pca*-Pol and its mutants was analyzed. No significant difference in the 3′-5′ exonuclease activity of wild-type enzyme and its three mutants was observed (Table 3). The wild-type and all its mutant enzymes (both single and double mutants) released the same amount of radioactivity (nearly 70 %) from the 3′-end of ^{3}H-

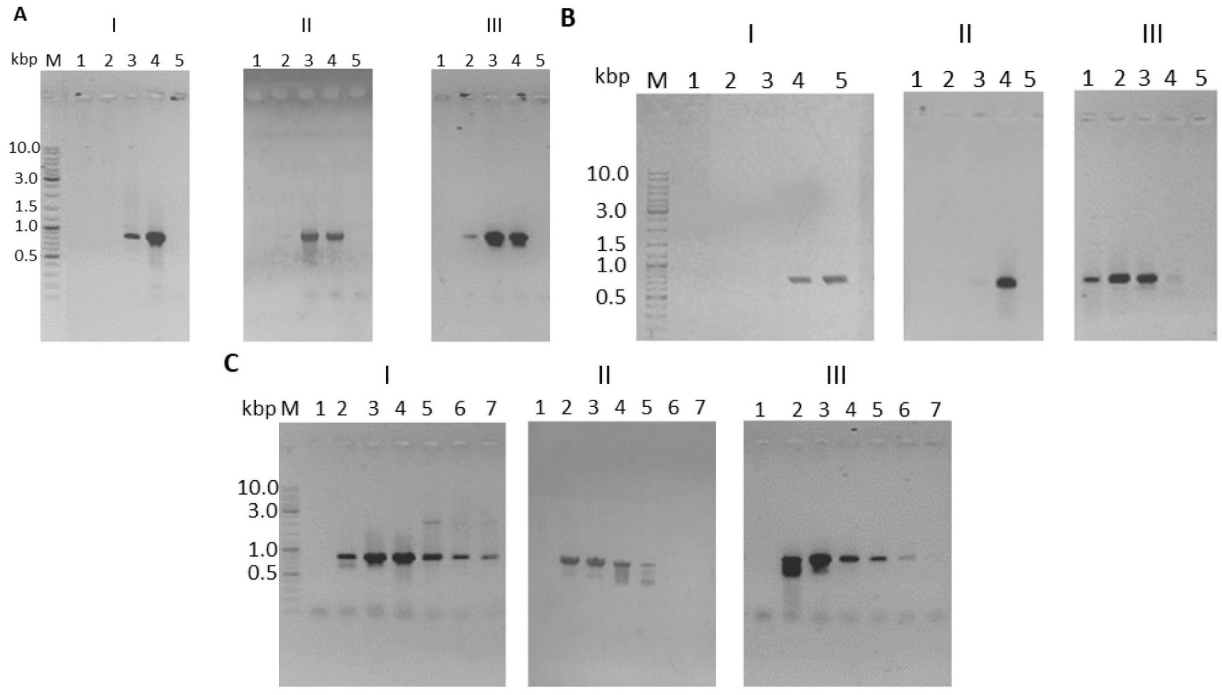

Fig. 3. A) Determination of optimum buffer pH for *Pca*-Pol mutants in PCR. I) Single mutant G522R. II) Single mutant E555R. III) Double mutant G522R-E555R. Lane M, molecular mass marker; lane 1, pH 7.0; lane 2, pH 7.5; lane 3, pH 8.0; lane 4, pH 8.5; lane 5, pH 9.0. B) Determination of optimum buffer concentration for *Pca*-Pol mutants in PCR. I) Single mutant G522R. II) Single mutant E555R. III) Double mutant G522R-E555R. Lane M, molecular mass marker; lane 1, 10 mM; lane 2, 20 mM; lane 3, 40 mM; lane 4, 60 mM; lane 5, 80 mM. C) Determination of optimum $MgCl_2$ concentration for *Pca*-Pol mutants in PCR. I) Single mutant G522R. II) Single mutant E555R. III) Double mutant G522R-E555R. Lane M, molecular mass marker; lane 1, 0 mM; lane 2, 1 mM; lane 3, 2 mM; lane 4, 4 mM; lane 5, 6 mM; lane 6, 8 mM; lane 7, 10 mM.

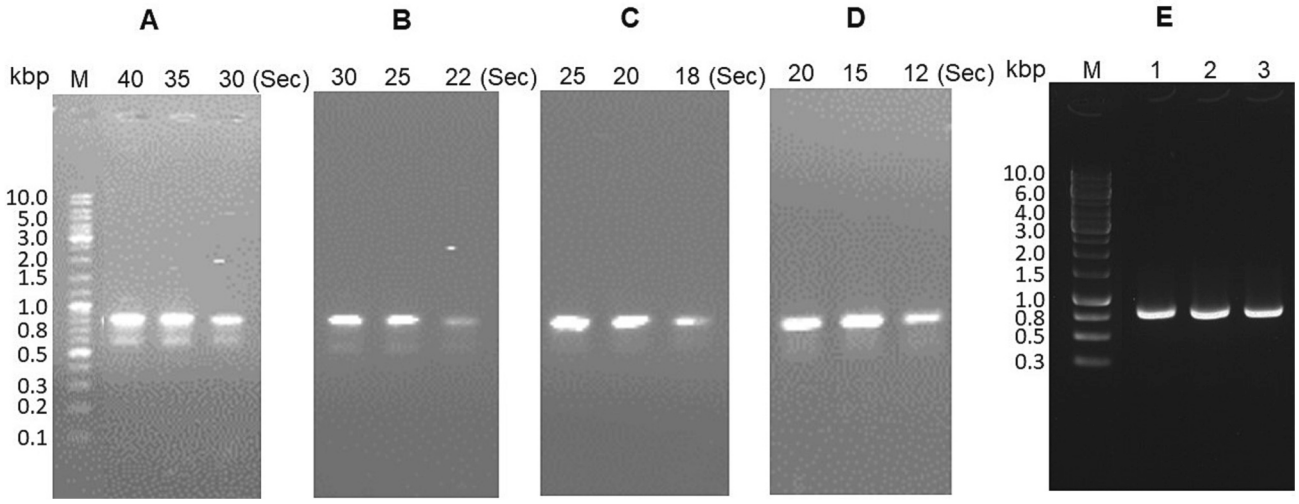

Fig. 4. Ethidium bromide stained agarose gel demonstrating comparison of PCR extension efficiency of wild-type *Pca*-Pol and its mutants. A) Wild-type; B) E555R; C) G522R; D) G552R-E555R. M, molecular mass marker. Extension time in seconds is shown on top of each lane. E) Comparison of PCR amplification by G522R-E555R and commercial DNA polymerases. Lane M, standard marker; lane 1, G522R-E555R; lane 2, *Pfu*; lane 3; *Taq*.

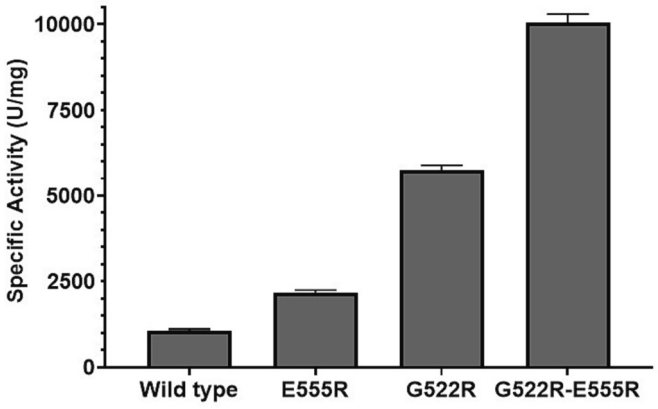

Fig. 5. Comparison of specific activities of wild-type *Pca*-Pol, its single mutants E555R and G522R, and double mutant G522R-E555R.

labeled DNA substrate. This indicated that all the mutants generated in this study retained 3′-5′ exonuclease activity in addition to an increase in their processivity as compared to that of wild-type *Pca*-Pol.

3.4.5. Analysis of fidelity

For fidelity analysis, pUC19 plasmid was PCR amplified by using different enzymes including wild-type *Pca*-Pol, G522R, E555R, G522R-

Table 2
Comparison of processivity[a] of wild-type *Pca*-Pol and its mutants with *Pfu* and KOD DNA polymerases.

Enzyme	Microscopic processivity (P_I)	Average primer extended length
Pfu	0.847 ± 0.02	6 ± 1
Wild-type	0.906 ± 0.002	9 ± 1
E555R	0.920 ± 0.004	12 ± 1
G522R	0.957 ± 0.004	23 ± 2
G522R-E555R	0.974 ± 0.002	38 ± 3
KOD	–	>300[b]

[a] Processivity is shown in terms of average primer extended length.
[b] Processivity of KOD DNA polymerase is reported from Takagi et al., 1997.

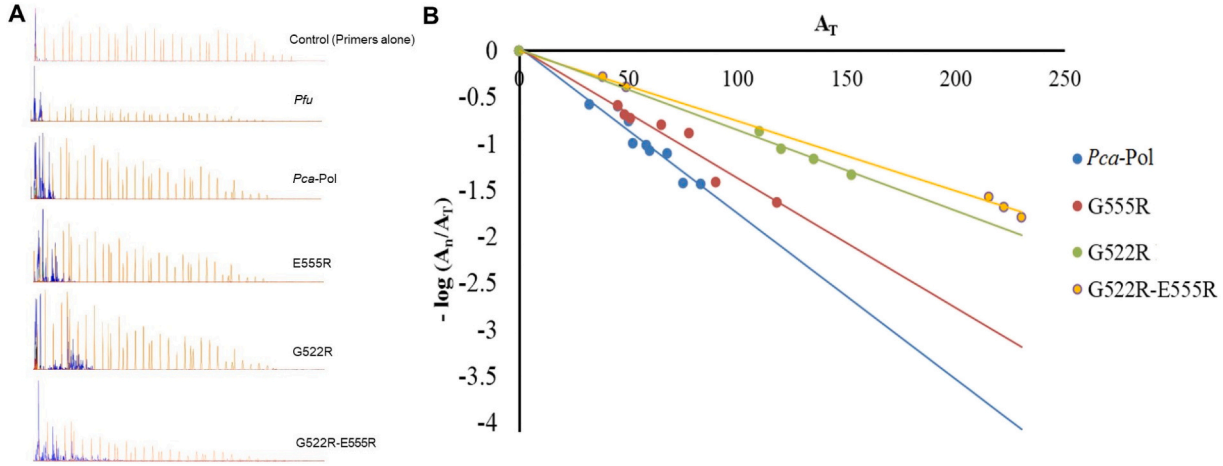

Fig. 6. A) Electropherogram traces of Primers, *Pfu*, *Pca*-Pol (wild-type), single mutant E555R, single mutant G522R and double mutant G522R-E555R DNA polymerases. Blue peaks in electropherogram correspond to single primer extension products and yellow peaks correspond to the standard LIZ600 size marker. B) Processivity of wild type *Pca*-Pol, single- and double-mutant DNA polymerases. Single primer extension products are plotted as log (A_{nt}/A_T) *versus* the length of extended primers and fitted by linear regression. A_{nt} and A_T represent the total extended fragments and the sum of the lengths of the extended primers.

Table 3
Exonuclease activity (3′-5′) of wild-type *Pcal*-Pol and its mutants.

Enzyme	Released radioactivity (cpm)
Wild-type	21,959 ± 19
G522R	21,735 ± 17
E555R	22,174 ± 21
G522R-E555R	21,689 ± 15

E555R, and *Pfu* DNA polymerases. After transformation, blue and white colonies on the selection plates were counted and error rate was determined. The error rate of these enzymes was: 2.7×10^{-6} (*Pfu*), 5.1×10^{-6} (wild-type *Pca*-Pol), 5.5×10^{-6} (G522R), 5.3×10^{-6} (E555R) and 5.8×10^{-6} (G522R-E555R) as shown in Table 4. Although, the fidelity of wild-type *Pca*-Pol and all mutant DNA polymerase was ~2-fold lower than that of the *Pfu* DNA polymerase but ~2-fold higher than that of *Taq* DNA polymerase [31]. All the three mutants generated in this study have fidelity similar to the wild-type enzyme *Pca*-Pol but showed improvement in their processivity.

4. Discussion

Many archaeal DNA polymerases have been characterized and used for biotechnological applications [32] and some have found commercial applications as well. However, virtually all commercial DNA polymerases are from the members of phylum euryarchaea [18]. The finger, palm and thumb domains of DNA polymerases are important for substrate binding and catalysis. Several studies have reported that modification of amino acids in these regions can improve the properties of DNA polymerases [29,31,33]. Also hybrid DNA polymerases have been shown to have improved properties and performance in PCR [20,34].

Processivity and fidelity are among the important properties of DNA polymerase. It has been reported that extension rate and processivity of DNA polymerases can be improved by coupling them to DNA binding proteins as a fusion protein [34–36]. In this connection, another important factor is the presence of positively charged amino acids which interact with bound DNA [19,37,38]. The DNA polymerase from *T. kodakarensis* (KOD DNA polymerase) has shown high processivity and extension rate in PCR [30]. Also it has been reported that presence of multiple positively charged amino acids in KOD DNA polymerase is important for DNA binding and catalysis [12]. Therefore, KOD DNA polymerase was used as a template to align and mutate *Pca*-Pol for improving its properties as the wild-type *Pca*-Pol exhibited relatively low processivity and extension rate [16]. Therefore, based on sequence alignment and structural analysis, a couple of mutations were introduced in *Pca*-Pol to improve its properties. The amino acid sequence of palm domain of *Pca*-Pol was aligned with that of KOD DNA polymerase. Arg501 of KOD DNA polymerase is an important positively charged amino acid at the fork point [19]. The corresponding amino acid of *Pca*-Pol was found to be Gly522. Similarly, Glu555 of *Pca*-Pol aligned with a conserved positively charged residue of other archaeal DNA polymerases. Therefore, both Gly522 and Glu555 of *Pca*-Pol were mutated to arginine, both as single mutants and a double mutant as well.

When the mutant models of *Pca*-Pol were analyzed by *in silico* analysis, it was found that both mutants were stable. In addition, *Pca*Arg522 mutant was predicted to form a salt bridge with Glu393 – whereas wild-type Gly522 does not have this interaction. Similarly *Pca*Arg555 mutant was predicted to form a hydrogen bond with Lys567. Moreover, the Arg555 mutant has greater solvent accessible area as compared to wild-type Glu555. Collectively, these factors can contribute to the observed improvement in stability and properties of the double mutant. Also *Pca*Arg555 lies close to metal binding aspartates of the palm domain. So it may possibly influence enzyme activity.

The primer extension ability of the double mutant, G522R-E555R, was more than 2-fold higher than that of the wild-type *Pca*-Pol. In addition, the amount of this double mutant required to produce same amount of DNA product by PCR was 8-fold lower than that of the wild-type. This value for the wild-type *Pca*-Pol was ~2-fold lower than that of *Pfu* DNA polymerase. Furthermore, this double mutant exhibited nearly 9-fold higher specific DNA polymerase activity as compared to the wild-type enzyme.

When compared with other commercial DNA polymerases, PCR extension ability of G522R-E555R double mutant was similar to that of *Pfu* and *Taq* DNA polymerases - both of which are routinely used DNA polymerases. However, the extension rate of G522R-E555R double mutant was more than its wild-type enzyme. Nonetheless, G522R-E555R double mutant exhibited better fidelity as compared to that of *Taq* DNA polymerase and could synthesize DNA more accurately.

In addition to processivity, the 3′- to 5′-exonuclease activity is pivotal for accurate copying of template by DNA polymerases. Wild-type *Pca*-Pol and its mutants generated in this study, possessed nearly same extent of 3′-5′ exonuclease activity. Because of the presence of 3′-5′ exonuclease activity, the error rate of wild-type *Pca*-Pol and its mutants was much lower than that of *Taq* DNA polymerase [18].

Many commercial DNA polymerases are available nowadays. *T. aquaticus* DNA polymerase and its variants are still widely used for PCR. Among archaeal DNA polymerases, all commercially available enzymes are of euarychaeal origin. KOD DNA polymerase, however, is superior in its properties with an elongation rate of more than hundred nucleotides/s and a processivity of around 300 bases [30]. Fork-point arginine residues of KOD DNA polymerase are important for DNA binding and enhanced processivity. Introduction of arginine residues on corresponding positions of *Pfu* DNA polymerase improved the properties of resulting variant [20]. Several studies have compared the performance of various commercial DNA polymerases (including both archaeal and bacterial DNA polymerases) and found *T. kodarensis*-based DNA polymerases to be more suitable for these PCR applications [39–41]. So, introducing arginine mutations in *Pca*-Pol has resulted in improving the properties of its resulting mutants. The double mutant G522R-E555R has better processivity and extension ability as compared to wild type *Pca*-Pol without affecting its fidelity. Moreover, the G522R-E555R double mutant showed better processivity and extension rate as compared to *Pfu* DNA polymerase – a widely used archaeal DNA polymerase.

Table 4
Comparison of fidelity of wild-type *Pca*-Pol and its mutants with *Pfu* DNA polymerase.

Enzyme	Blue colonies	White colonies	Mutation frequency (mf)	Template doubling (d)	Error rate ($\times 10^{-6}$)
Pfu	6171 ± 118	36 ± 2	0.006 ± 0.002	7 ± 0.3	2.7 ± 0.2
Pca-Pol	5697 ± 109	72 ± 4	0.012 ± 0.0002	7 ± 0.1	5.1 ± 0.3
G522R	6235 ± 120	79 ± 5	0.012 ± 0.001	7 ± 0.4	5.5 ± 0.3
E555R	5974 ± 113	76 ± 5	0.012 ± 0.0003	7 ± 0.5	5.3 ± 0.3
G522R-E555R	6814 ± 126	93 ± 6	0.013 ± 0.0005	7 ± 0.2	5.8 ± 0.2

5. Conclusion

Replacement of non-polar (Gly522) and negatively charged (Glu555) residues with positively charged arginine in the palm domain resulted in increased substrate affinity. The double mutant enzyme, G522R-E555R, exhibited ~9-fold higher specific activity than that of the wild-type. Processivity of G522R-E555R was ~4-fold higher than that of the wild-type. Error rate of G522R-E555R mutant was nearly same as that of the wild-type despite an increase in processivity. The extension ability of this mutant was equivalent to commercially available *Taq* DNA polymerase while double than that of the wild-type *Pca*-Pol and *Pfu* DNA

polymerase. These improved features make G522R-E555R a potential candidate for applications in PCR.

Declaration of competing interest

The authors declare that they have no competing interests.

Acknowledgment

The authors wish to thank Higher Education Commission of Pakistan for providing support.

Appendix A. Supplementary data

Supplementary data to this article can be found online at https://doi.org/10.1016/j.ijbiomac.2023.123545.

References

[1] I. Geronimo, P. Vidossich, E. Donati, M. De Vivo, Computational investigations of polymerase enzymes: structure, function, inhibition, and biotechnology, WIREs Comput. Mol. Sci. 11 (2021), e1534, https://doi.org/10.1002/wcms.1534.
[2] J. Aschenbrenner, A. Marx, DNA polymerases and biotechnological applications, Curr. Opin. Biotechnol. 48 (2017) 187–195, https://doi.org/10.1016/j.copbio.2017.04.005.
[3] L. Zhang, M. Kang, J. Xu, Y. Huang, Archaeal DNA polymerases in biotechnology, Appl. Microbiol. Biotechnol. 99 (2015) 6585–6597, https://doi.org/10.1007/s00253-015-6781-0.
[4] A. Nikoomanzar, N. Chim, E.J. Yik, J.C. Chaput, Engineering polymerases for applications in synthetic biology, Q. Rev. Biophys. 53e8 (2020) 1–31, https://doi.org/10.1017/S0033583520000050.
[5] C. Samson, P. Legrand, M. Tekpinar, J. Rozenski, M. Abramov, P. Holliger, V. B. Pinheiro, P. Herdewijn, M. Delarue, Structural studies of HNA substrate specificity in mutants of an archaeal DNA polymerase obtained by directed evolution, Biomolecules 10 (2020) 1647, https://doi.org/10.3390/biom10121647.
[6] P.M. Burgers, E.V. Koonin, E. Bruford, L. Blanco, K.C. Burtis, M.F. Christman, W. C. Copeland, E.C. Friedberg, F. Hanaoka, D.C. Hinkle, C.W. Lawrence, M. Nakanishi, H. Ohmori, L. Prakash, S. Prakash, C.A. Reynaud, A. Sugino, T. Todo, Z. Wang, J.C. Weill, R. Woodgate, Eukaryotic DNA polymerases: proposal for a revised nomenclature, J. Biol. Chem. 276 (2001) 43487–43490, https://doi.org/10.1074/jbc.R100056200.
[7] D. Kazlauskas, M. Krupovic, J. Guglielmini, P. Forterre, Č. Venclovas, Diversity and evolution of B-family DNA polymerases, Nucleic Acids Res. 48 (2020) 10142–10156, https://doi.org/10.1093/nar/gkaa760.
[8] M.D. Greci, S.D. Bell, Archaeal DNA replication, Annu. Rev. Microbiol. 8 (2020) 65–80, https://doi.org/10.1146/annurev-micro-020518-115443.
[9] C.D.O. Cooper, Archaeal DNA polymerases: new frontiers in DNA replication and repair, Emerg. Top.Life Sci. 14 (2018) 503–516, https://doi.org/10.1042/ETLS20180015.
[10] L. Zhang, D. Jiang, H. Shi, M. Wu, Q. Gan, Z. Yang, P. Oger, Characterization and application of a family B DNA polymerase from the hyperthermophilic and radioresistant euryarchaeon Thermococcus gammatolerans, Int. J. Biol. Macromol. 1 (2020) 217–224, https://doi.org/10.1016/j.ijbiomac.2020.03.204.
[11] S.J. Firbank, J. Wardle, P. Heslop, R.J. Lewis, B.A. Connolly, Uracil recognition in archaeal DNA polymerases captured by X-ray crystallography, J. Mol. Biol. 381 (2008) 529–539, https://doi.org/10.1016/j.jmb.2008.06.004.
[12] K. Bergen, K. Betz, W. Welte, K. Diederichs, A. Marx, Structures of KOD and 9 degrees N DNA polymerases complexed with primer template duplex, Chembiochem. 14 (2013) 1058–1062, https://doi.org/10.1002/cbic.201300175.
[13] Y. Weng, X. Liu, Characterization of a family B DNA polymerase from Thermococcus eurythermalis A501 and its application in PCR, Sheng Wu Gong Cheng Xue Bao 38 (2022) 807–819, https://doi.org/10.13345/j.cjb.210095.
[14] S.W. Kim, D.U. Kim, J.K. Kim, L.W. Kang, H.S. Cho, Crystal structure of Pfu, the high fidelity DNA polymerase from Pyrococcus furiosus, Int. J. Biol. Macromol. 42 (2008) 356–361, https://doi.org/10.1016/j.ijbiomac.2008.01.010.
[15] J. Guo, W. Zhang, A.R. Coker, S.P. Wood, J.B. Cooper, S. Ahmad, S.F. Ali, N. Rashid, M. Akhtar, Structure of the family B DNA polymerase from the hyperthermophilic archaeon Pyrobaculum calidifontis, Acta Crystallogr.Sect.D Struct. Biol. 73 (2017) 420–427, https://doi.org/10.1107/S2059798317004090.
[16] S.F. Ali, N. Rashid, T. Imanaka, M. Akhtar, Family B DNA polymerase from a hyperthermophilic archaeon Pyrobaculum calidifontis: cloning, characterization and PCR application, J. Biosci. Bioeng. 2 (2011) 118–123, https://doi.org/10.1016/j.jbiosc.2011.03.018.
[17] F.M. Pisani, C. De Martino, M. Rossi, A DNA polymerase from the archaeon Sulfolobus solfataricus shows sequence similarity to family B DNA polymerases, Nucleic Acids Res. 11 (1992) 2711–2716, https://doi.org/10.1093/nar/20.11.2711.
[18] K. Terpe, Overview of thermostable DNA polymerases for classical PCR applications: from molecular and biochemical fundamentals to commercial systems, Appl. Microbiol. Biotechnol. 97 (2013) 10243–10254, https://doi.org/10.1007/s00253-013-5290-2.
[19] H. Hashimoto, M. Nishioka, S. Fujiwara, M. Takagi, T. Imanaka, T. Inoue, Y. Kai, Crystal structure of DNA polymerase from hyperthermophilic archaeon Pyrococcus kodakarensis KOD1, J. Mol. Biol. 306 (2001) 469–477, https://doi.org/10.1006/jmbi.2000.4403.
[20] A.M. Elshawadfy, B.J. Keith, H.E. Ooi, T. Kinsman, P. Heslopand, B.A. Connolly, DNA polymerase hybrids derived from the family-B enzymes of Pyrococcus furiosus and Thermococcus kodakarensis: improving performance in the polymerase chain reaction, Front. Microbiol. 5 (2014) 224, https://doi.org/10.3389/fmicb.2014.00224.
[21] S. Ahmad, S.F. Ali, N. Azim, N. Rashid, Studies on enhancement of production of recombinant DNA polymerase originated from Pyrobaculum calidifontis, Biologia 76 (2021) 3579–3586, https://doi.org/10.1007/s11756-021-00887-7.
[22] B. Webb, A. Sali, Comparative protein structure modeling using Modeller, in: Current Protocols in Bioinformatics 54, John Wiley & Sons, Inc., 2016, pp. 5.6.1–5.6.37, https://doi.org/10.1002/cpbi.3.
[23] S. Kumar, C.J. Tsai, B. Ma, R. Nussinov, Contribution of salt bridges toward protein thermostability, J. Biomol. Struct. Dyn. 1 (2000) 79–86, https://doi.org/10.1080/07391102.2000.10506606.
[24] L. Willard, A. Ranjan, H. Zhang, H. Monzavi, R.F. Boyko, B.D. Sykes, D.S. Wishart, VADAR: a web server for quantitative evaluation of protein structure quality, Nucleic Acids Res. 31 (2003) 3316–3319, https://doi.org/10.1093/nar/gkg565.
[25] J. Schymkowitz, J. Borg, F. Stricher, R. Nys, F. Rousseau, L. Serrano, The FoldX web server: an online force field, Nucleic Acids Res. 33 (2005) W382–W388, https://doi.org/10.1093/nar/gki387.
[26] J.P.D. Goldring, Measuring protein concentration with absorbance, Lowry, Bradford Coomassie Blue, or the Smith Bicinchoninic acid assay before electrophoresis, Methods Mol. Biol. 2019 (1855) 31–39, https://doi.org/10.1007/978-1-4939-8793-1_3.
[27] Y. Wang, D. Prosen, L. Mei, J.C. Sullivan, M. Finney, P.B. Vander Horn, A novel strategy to engineer DNA polymerases for enhanced processivity and improved performance in vitro, Nucleic Acids Res. 32 (2004) 1197–1207, https://doi.org/10.1093/nar/gkh271.
[28] A. Saghatelyan, H. Panosyan, A. Trchounian, N.K. Birkeland, Characteristics of DNA polymerase I from an extreme thermophile, Thermus scotoductus strain K1, MicrobiologyOpen 10 (2021), e1149, https://doi.org/10.1002/mbo3.1149.
[29] H. Ppyun, S.H. Kim, M.H. Youn, S.S. Cho, K.M. Kwon, D.H. Kweon, S.T. Kwon, Improved PCR performance and fidelity of double mutant Neq A523R/N540R DNA polymerase, Enzym. Microb. Technol. 82 (2016) 197–204, https://doi.org/10.1016/j.enzmictec.2015.10.010.
[30] M. Takagi, M. Nishioka, H. Kakihara, M. Kitabayashi, H. Inoue, B. Kawakami, M. Oka, T. Imanaka, Characterization of DNA polymerase from Pyrococcus sp. strain KOD1 and its application to PCR, Appl. Environ. Microbiol. 63 (1997) 4504–4510, https://doi.org/10.1128/aem.63.11.4504-4510.1997.
[31] K.P. Kim, S.S. Cho, K.K. Lee, M.H. Youn, S.T. Kwon, Improved thermostability and PCR efficiency of Thermococcus celericrescens DNA polymerase via site-directed mutagenesis, J. Biotechnol. 155 (2011) 156–163, https://doi.org/10.1016/j.jbiotec.2011.06.022.
[32] S. Ishino, Y. Ishino, DNA polymerases as useful reagents for biotechnology - the history of developmental research in the field, Front. Microbiol. 5 (2014) 465, https://doi.org/10.3389/fmicb.2014.00465.
[33] H. Ppyun, I. Kim, S.S. Cho, K.J. Seo, K. Yoon, S.T. Kwon, Improved PCR performance using mutant tpa-S DNA polymerases from the hyperthermophilic archaeon Thermococcus pacificus, J. Biotechnol. 164 (2012) 363–370, https://doi.org/10.1016/j.jbiotec.2013.01.022.
[34] M. Olszewski, M. Śpibida, M. Bilek, B. Krawczyk, Fusion of Taq DNA polymerase with single-stranded DNA binding-like protein of Nanoarchaeum equitans – expression and characterization, PLoS ONE 12 (2017), e0184162, https://doi.org/10.1371/journal.pone.0184162.
[35] J. Wu, A. de Paz, B.M. Zamft, A.H. Marblestone, E.S. Boyden, K.P. Kording, K.E. J. Tyo, DNA binding strength increases the processivity and activity of a Y-Family DNA polymerase, Sci. Rep. 7 (2017) 4756, https://doi.org/10.1038/s41598-017-02578-3.
[36] M. Śpibida, B. Krawczyk, M. Olszewski, J. Kur, Modified DNA polymerases for PCR troubleshooting, J. Appl. Genet. 58 (2017) 133–142, https://doi.org/10.1007/s13353-016-0371-4.
[37] G. Rodríguez, M.T. Martín, M. de Vega, An array of basic residues is essential for the nucleolytic activity of the PHP domain of bacterial/archaeal PolX DNA polymerases, Sci. Rep. 9 (2019) 9947, https://doi.org/10.1038/s41598-019-46349-8.
[38] K. Kasho, G. Stojkovič, C. Velázquez-Ruiz, M.I. Martínez-Jiménez, M. Doimo, T. Laurent, A. Berner, A.E. Pérez-Rivera, L. Jenninger, L. Blanco, S. Wanrooij, A unique arginine cluster in PolDIP2 enhances nucleotide binding and DNA synthesis by PrimPol, Nucleic Acids Res. 49 (2021) 2179–2191, https://doi.org/10.1093/nar/gkab049.
[39] S. Nagai, S. Sildever, N. Nishi, S. Tazawa, L. Basti, T. Kobayashi, Y. Ishino, Comparing PCR-generated artifacts of different polymerases for improved accuracy

of DNA metabarcoding, Metabarcoding Metagenom. 6 (2022), e77704, https://doi.org/10.3897/mbmg.6.77704.

[40] T. Sittivicharpinyo, P. Wonnapinij, W. Surat, Efficiency comparison of four high-fidelity DNA polymerases for dengue virus detection and genotype identification in field-caught mosquitoes, Agric.Nat. Resour. 52 (2018) 84–92, https://doi.org/10.1016/j.anres.2018.05.012.

[41] M. Miura, C. Tanigawa, Y. Fujii, S. Kaneko, Comparison of six commercially-available DNA polymerases for direct PCR, Rev. Inst. Med. Trop. Sao Paulo 55 (2013) 401–406, https://doi.org/10.1590/S0036-46652013000600005.